Vertical partitions in slender rectangular cavities

Edwin S. Nowak and Milos H. Novak
Faculty of Engineering Science, University of Western Ontario, Ontario, Canada

Two-dimensional laminar natural convection heat transfer in slender rectangular cavities equipped with two small vertical partitions, located in the middle of horizontal walls, is studied numerically. The evaluations are carried out for cavity aspect ratios up to 45 and for Grashof numbers, based on the cavity height, up to 5×10^8. As shown, for this range of aspect ratios and Grashof numbers, two small vertical partitions of the same length, made of glass and located in the mid-plane of the cavity, may reduce the cavity mean as well as peak Nusselt numbers by up to 6 and 27 percent, respectively.

Keywords: natural convection; numerical methods

Introduction

Many numerical works of natural convection heat transfer in square cavities or in rectangular cavities with lower aspect ratios have been published until present. In the original works of Wilkes and Churchill (1966), Newell and Schmidt (1970) and Chu and Churchill (1977) researchers chose the vorticity-stream function approach to solve (using the finite-difference techniques) the vorticity, energy and stream function equations. Because of the suitability for numerical solution this approach has been adopted later in several numerical studies.

For slender rectangular cavities, very interesting works of Korpela et al. (1982) and of Lee and Korpela (1983) were published. In both studies authors describe the fluid-flow regimes (transition, multicellular and conduction) occurring in slender rectangular cavities. As a function of the Grashof and Prandtl numbers the cavity heat transfer and fluid-flow distributions are discussed for aspect ratios ranging from 10–40. Primarily the study of Lee and Korpela (1983) gives the detailed description of the multicellular fluid-flow regime, which may be developed in slender cavities as the consequence of the hydrodynamic instability (Bergholz 1978). In this, for slender cavities very common regime, the heat is transferred along the finite number of convection cells. Provided that the Grashof number is sufficiently high, the occurrence of these cells may be expected in the air cavities with aspect ratios, $R = H/L \geq 12$.

Closely related to the present study are some results of both experimental and numerical investigations on cavity with vertical partitions, located on the cavity horizontal walls, which were published. In 1982 Bejan presented a numerical study aimed at the determination of how both horizontal and vertical internal obstructions may affect the cavity heat transfer for aspect ratios, R, ranging from 0.5–10. Compared with the cavity without any internal obstruction in which the convection-dominated regime exists, it is shown that the vertical diathermal partition may reduce the heat-transfer rate by 50 percent. For the case of square cavity, the numerical study of Zimmerman and Acharya (1987) describes the effect of finitely conducting buffels attached on cavity horizontal walls on the cavity heat transfer. They also compared their numerical finite-difference results with the experimental data of Bajorek and Lloyd (1982), and found that numerical and experimental data agreed well for perfectly conducting end walls. The significant discrepancy was encountered for adiabatic end-wall assumptions. Following work of Jetli and Acharya (1988) shows how different location and height of inner vertical partitions affect the cavity

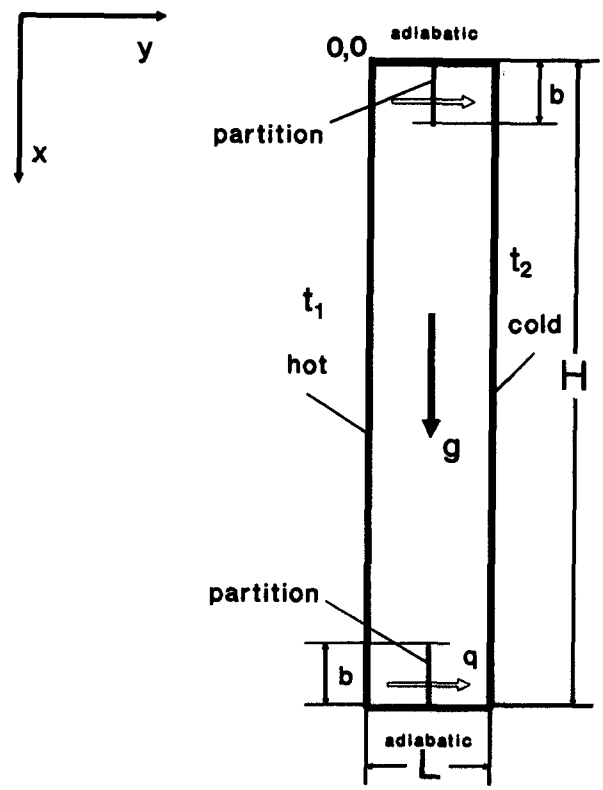

Figure 1 Scheme of the rectangular cavity with two vertical partitions located in the middle of the cavity end walls

Address reprint requests to Dr. Novak at the Faculty of Engineering Science, University of Western Ontario, Ontario, Canada, N6A5B9.

Received 21 February 1993; accepted 10 October 1993

heat transfer. This study also describes the effect of different boundary conditions imposed on horizontal walls on cavity, Nusselt number and fluid-flow distribution. Finally, the work of Ciofalo and Karayiannis (1991) describes the effect of symmetric partitions protruding centrally from the cavity end walls on heat-transfer rates. The results are achieved for the Rayleigh number ranging from 10^4–10^7, cavity aspect ratios from 0.5–10 and for the variable partition height ranging from 0–50 percent (two separate enclosures) of the total cavity height.

Despite the many articles published in this field, no theoretical studies, dealing primarily with the suppression of the convection heat-transfer peaks occurring near the cavity top and bottom, have been published. Insufficient heat-transfer resistance in this area, especially in the lower part of the double-paned window cavity, allows the formation of condensation on the inside window pane. This is a phenomenon that considerably affects the window heat loss as well as the durability of wooden frames.

The goal of this work is to determine numerically the effect of convection barriers (partitions), located in the mid-plane of the air cavity, on the cavity heat-transfer performance and, especially, on the local Nusselt number distribution. The numerical finite-difference approach was chosen and efficiently programmed to solve the Navier-Stokes equations and to investigate the temperature contours, stream lines and the local Nusselt number distribution inside a vertical air-filled cavity. As evaluated, under certain conditions, just small glass partitions may appreciably suppress the peak heat-transfer coefficient in the cavity. The higher local resistance will cause a new temperature distribution across the window and, consequently, will lead to possible elimination of the condensation formation on the inside window surface.

Problem description

To obtain temperature and stream pattern profiles in the cavity, the Navier-Stokes equations, in simplified form with Boussinesq approximation involved, are solved numerically. The pressure elimination from the equations of motion leads to the well-known system of dimensionless equations for vorticity, energy and the stream function, that is,

$$\frac{\partial \Omega}{\partial \tau} + U\frac{\partial \Omega}{\partial X} + V\frac{\partial \Omega}{\partial Y} = \mathrm{Gr}\frac{\partial \Theta}{\partial Y} + \frac{\partial^2 \Omega}{\partial X^2} + \frac{\partial^2 \Omega}{\partial Y^2} \tag{1}$$

$$U\frac{\partial \Theta}{\partial X} + V\frac{\partial \Theta}{\partial Y} = \frac{1}{\mathrm{Pr}}\left(\frac{\partial^2 \Theta}{\partial X^2} + \frac{\partial^2 \Theta}{\partial Y^2}\right) \tag{2}$$

$$-\Omega = \frac{\partial^2 \Psi}{\partial X^2} + \frac{\partial^2 \Psi}{\partial Y^2} \tag{3}$$

where,

$$U = \frac{\partial \Psi}{\partial Y};\ V = -\frac{\partial \Psi}{\partial X}$$

In the preceding equations the *dimensionless variables* are defined as follows:

- Cartesian coordinates in the vertical direction, $X = x/H$, and in the horizontal direction, $Y = y/H$
- Vorticity, $\Omega = H^2\omega/\nu$
- Temperature, $\Theta = (t - t_2)/(t_1 - t_2)$
- Velocity in the vertical, X, direction, $U = Hu/\nu$
- Velocity in the horizontal, Y, direction, $V = Hv/\nu$
- Stream function, $\Psi = \psi/\nu$
- Time, $\tau = \tau^*\nu/H^2$

Based on these definitions, the corresponding boundary conditions for the rectangular cavity, depicted in Figure 1, can be expressed in dimensionless form.

1. $\tau = 0 \ldots \Theta = \Theta_0,\ \Omega = \Omega_0,\ U = V = 0,\ \Psi = \Psi_0$
2. $\tau > 0 \ldots$

$\partial\Theta/\partial X = U = V = 0$ for $X = 0,\ 0 \le Y \le L/H$

$\partial\Theta/\partial X = U = V = 0$ for $X = 1,\ 0 \le Y \le L/H$

$\Theta = 1$ and $U = V = 0$ for $0 \le X \le 1,\ Y = 0$

$\Theta = 0$ and $U = V = 0$ for $0 \le X \le 1,\ Y = L/H$

For the partition region:

$U = V = 0$, and the energy balance for the (very thin vertical) partition:

$$\partial\Theta/\partial Y)_{\mathrm{LEFT}} = K\partial\Theta/\partial Y)_{\mathrm{PART}} = \partial\Theta/\partial Y)_{\mathrm{RIGHT}}$$

$K = k_p/k$ denotes the partition-air conductivity ratio, LEFT RIGHT describe heat flux at the partition interface and PART is related to the heat flux through the partition itself in the horizontal, Y, direction.

Notation

b	partition height, in percent of the total cavity height H
Gr	Grashof number based on the cavity height = $g\beta(t_1 - t_2)H^3/\nu^2$
g	gravitational acceleration
H	cavity height
h	peak convection heat-transfer coefficient
h_{mean}	mean convection heat-transfer coefficient
$k(k_p)$	air (partition) thermal conductivity
L	cavity width
Nu	peak Nusselt number in the cavity with two partitions based on the cavity height
Nu_{max}	peak Nusselt number in the simple cavity without partitions based on the cavity height
Nu_{mean}	mean Nusselt number based on cavity height = hH/k
Pr	Prandtl number
R	cavity aspect ratio = H/L
t	fluid temperature
$t_{1(2)}$	hot (cold) side-wall temperature
$u(U)$	dimensional (dimensionless) velocity component in the vertical direction
$v(V)$	dimensional (dimensionless) velocity component in the horizontal direction
$x(X)$	dimensional (dimensionless) Cartesian coordinates in the vertical direction
$y(Y)$	dimensional (dimensionless) Cartesian coordinates in the horizontal direction

Greek letters

β	volumetric thermal expansion coefficient
Θ	dimensionless temperature
ν	kinematic viscosity
$\psi(\Psi)$	dimensional (dimensionless) stream function
$\tau^*(\tau)$	dimensional (dimensionless) time
$\omega(\Omega)$	dimensional (dimensionless) vorticity

Analysis

The task solved by the program is geometrically symmetrical. This makes numerical calculations faster and more accurate. In all cases evaluated, the cavity horizontal walls (top and bottom) are considered to be adiabatic and vertical walls isothermal. The partitions are located in the middle of the horizontal walls, their thickness is equal to the step size in the horizontal, Y, direction (1/32 of the cavity width L) and are made of glass. Both partitions have an equal height (length), b, expressed in percent of the total cavity height, H.

Local Nusselt numbers are evaluated from the definition in the form $\mathrm{Nu} = hH/k = \partial\Theta/\partial Y)_{\mathrm{wall}}$, and the cavity mean Nusselt number is determined using the Simpson rule to integrate the local Nusselt numbers along the cavity side walls. The detailed validation of the methodology used and the computational accuracy is given in Novak and Nowak (1993); consequently, just brief note is given here.

Based on several tests with various grid densities, the 202 × 32 grid was chosen to represent both the fluid-flow pattern, the cavity peak and mean Nusselt numbers. An extrapolation study showed that the evaluation error should be less than 10 and 2 percent for the peak and mean Nusselt numbers, respectively. Residual errors in steady state were evaluated at each grid point for all equations solved. For the temperature equation, the value of the maximum residue divided by the smallest equation term at the same grid point did not exceed 5.6/105. Under these conditions, the difference between the mean Nusselt numbers evaluated independently for the hot and cold vertical walls never exceeded 0.5 percent. Regardless of initial conditions, it was found that the solution is unique and stable for a simple rectangular cavity without partitions. However, for a cavity with two small partitions (of height up to 5 percent of H) and the multicellular fluid flow regime, the steady-state multicellular flow pattern (number of vortices) can be slightly affected by the initial conditions. Nevertheless, this happened only twice and, in addition to it, nearly no changes either in the cavity peak or mean Nusselt number values were observed. For this reason this effect will not be further pursued in this article.

As there are no available results known to the authors of this work on slender cavities ($R > 15$) with partitions, the present calculations are, in Figure 2, compared against available data for the case of the simple cavity without partitions. In Figure 2 the mean Nusselt number, $\mathrm{Nu}_{\mathrm{mean}} = h_{\mathrm{mean}}H/k$, is shown as

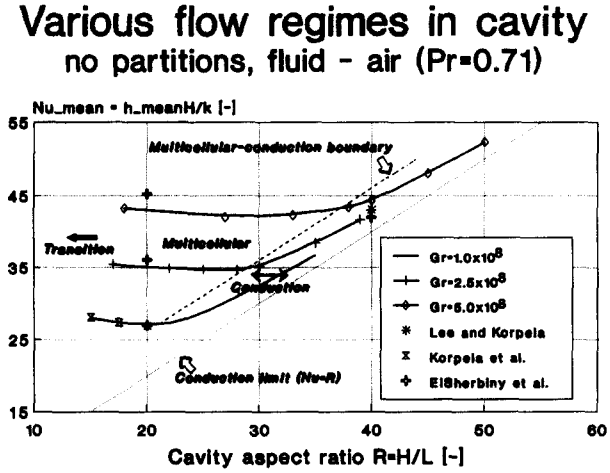

Figure 2 Mean Nusselt numbers in the cavity without inner partitions

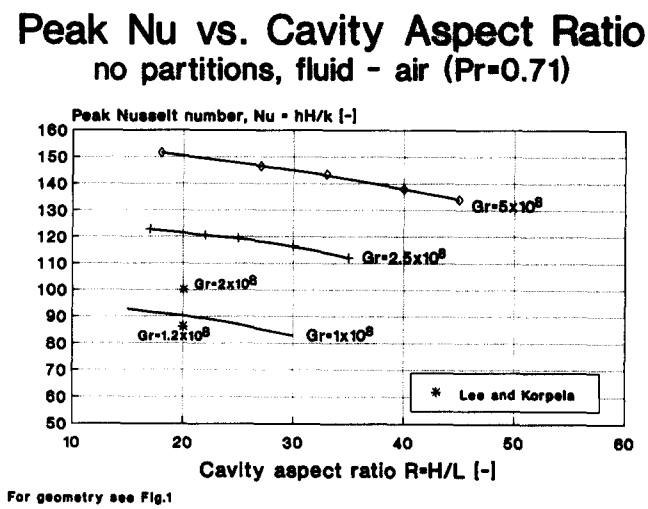

Figure 3 Peak Nusselt numbers in the cavity without inner partitions

a function of the cavity aspect ratio, $R = H/L$, with the Grashof number based on the cavity height, $\mathrm{Gr} = g\beta(t_1 - t_2)H^3/\nu^2$, as a parameter. The comparison of present calculations with numerical data of Korpela et al. (1982) and Lee and Korpela (1983) shows a very good agreement between results achieved. Some of the experimental measurements by ElSherbiny et al. (1982) on the cavity with highly conducting top and bottom, for aspect ratios, R, ranging from 5–110 are also depicted in Figure 2. As shown, their experimental data do not differ from present numerical results by more than 5 percent. Compared with ElSherbiny's experimental results, all numerical calculations reported here were performed on the cavity with the adiabatic top and bottom. However, as proved by numerous calculations, for the range of aspect ratios investigated, different boundary conditions imposed on horizontal cavity walls do not affect the cavity mean Nusselt number by more than 4 percent. Figure 2 also shows the various fluid flow regimes that may exist in slender cavities. In the conduction regime, the narrower the cavity is the higher the heat transfer through this cavity. Sufficiently far from the multicellular-conduction boundary in the conduction regime, the heat transfer approaches the *conduction limit* with the mean Nusselt number given only as a function of the cavity aspect ratio, $\mathrm{Nu}_{\mathrm{mean}} = R$. Contrarily, in the multicellular regime, the mean Nusselt number strongly depends on the Grashof number value but near the multicellular-conduction boundary remains almost unaffected by the cavity aspect ratio change.

Figure 3 shows the cavity peak (local maximum) Nusselt numbers for the same aspect ratios and Grashof numbers as in Figure 2. The comparison of present calculations on 202 × 32 grid with two available numerical values of Lee and Korpela (1983) on 129 × 17 grid shows that their data fall below present peak Nusselt numbers. This discrepancy is probably because of the different grid sizes in the vertical direction (Lee and Korpela 129, present study 202), from which the peak Nusselt number is strongly dependent.

Results

To examine how two glass partitions, both of the same height, b, located in the middle of cavity horizontal walls, affect the fluid flow and temperature distribution, the partition boundary conditions (see problem description) were imposed on the program calculations. As the task is symmetrical along the

cavity centerpoint, just the fluid flow at the one partition vicinity is discussed further.

The results, for both the so-called multicellular and the conduction regimes, are shown in Figures 4 and 5, respectively.

Figure 4 gives detailed information of how the variable height of partition b (b = 0, 5, 10 or 20 percent of H) changes the multicellular fluid flow structure inside the cavity. As already mentioned, this regime exists as the consequence of the hydrodynamic instability, and the heat is transferred along the finite number of convection cells. The comparison of Figures 4b–d indicates that the number of these cells is affected by the partition height. The higher the partition is, the more obvious the flow pattern change. The partition apparently squeezes the cavity height, and pushes the fluid-flow pattern from multicellular to the unicellular transition regime (Figure 4d). The zoomed views of local Nusselt numbers depicted in Figure 4 show that the partition reduces the cavity peak Nusselt number (approximately by 30 percent) and shifts the peak

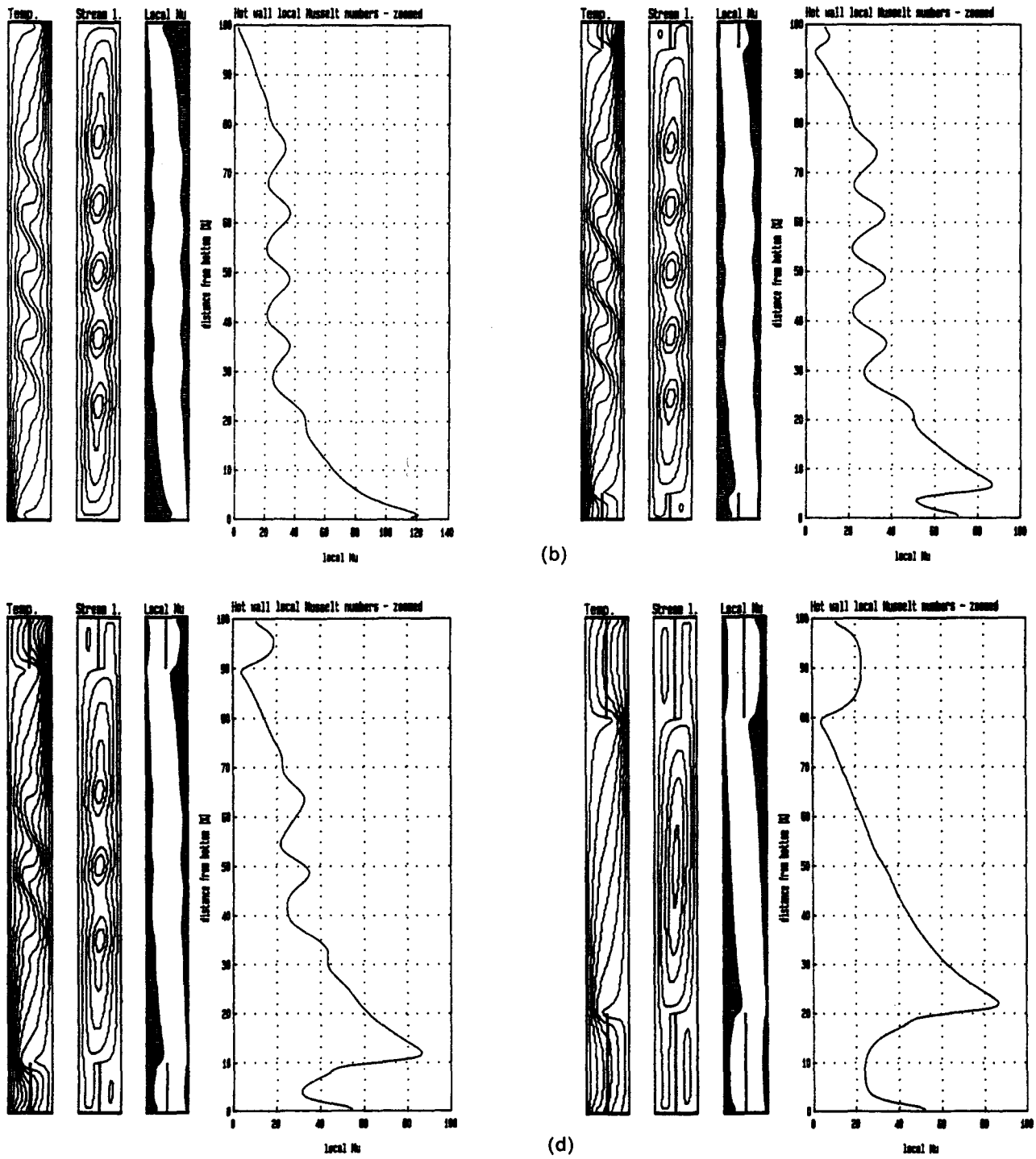

Figure 4 Temperature, stream lines and local Nusselt numbers in the cavity with two thin glass partitions located in the middle of end walls; Gr = 2.5 × 10^8, R = 22, and the height of partitions, b, equal of (a) b = 0%, (b) b = 5%, (c) b = 10% or (d) b = 20% of the total cavity height H

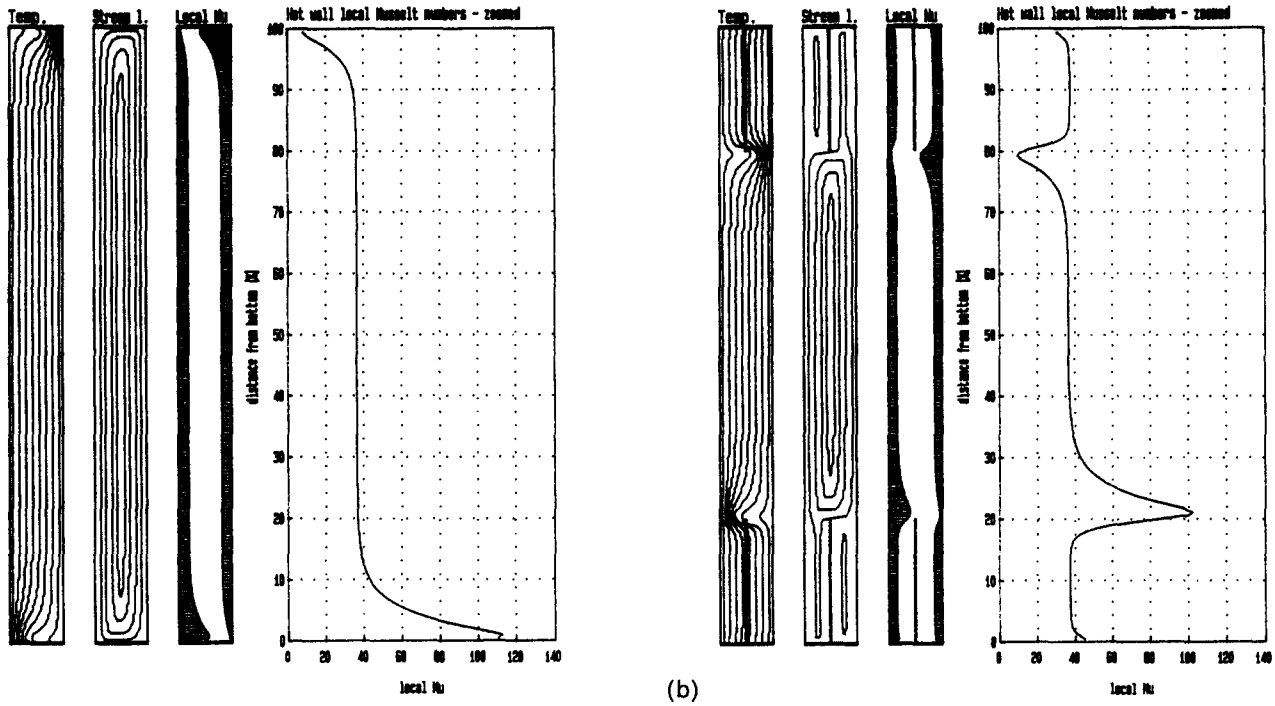

Figure 5 Temperature, stream lines and local Nusselt numbers in the cavity with two very thin glass partitions located in the middle of end walls; Gr = 2.5 × 10^8, $R = 35$ and the height of partitions, b, equal of (a) $b = 0\%$, (b) $b = 20\%$ of the total cavity height H

heat-transfer area from the cavity horizontal wall to the partition top. The shapes of isotherms also suggest that the heat transfer at the partition vicinity is very similar to that described by the conduction fluid-flow regime with very low flow velocities developed.

The fluid-flow distributions in cavities with existing conduction flow regime are shown in Figure 5.

Figure 5a depicts the simple rectangular cavity without inner partitions, and Figure 5b shows the cavity equipped with two inner partitions both of the same height, $b = 20$ percent of H. The comparison of these figures suggests that, in the conduction regime, the partition only shifts the maximum heat-transfer area away from the cavity horizontal surface to the partition top and nearly does not affect the peak Nusselt number value. Although not shown, these conclusions are valid for shorter partitions ($b \leq 20$ percent of H) too. In addition to it, the comparison of Figures 5a and b also shows that even these long partitions (20 percent of H) do not change the conduction fluid-flow structure existing in the cavity; that is, no noticeable change in the location of the multicellular-conduction boundary (see Figure 2), resulting from the partition presence, was observed.

Compared with the simple cavity without partitions, it was further evaluated that, in the multicellular (Figures 4a–c) or in the transition regime (Figure 4d), two small partitions both of the same height ($b \leq 10$ percent of H) decrease the mean Nusselt number value by up to 6 percent. However, in the conduction fluid flow regime (Figure 5), the change of the mean Nusselt number, as the consequence of partition presence, is negligible. Corresponding dependencies are depicted in Figure 6. As numerous calculations and also the detailed comparison of Figures 2 and 6 suggest, for cavities with aspect ratios higher than the conduction-multicellular boundary indicates (conduction regime), the effect of partitions on the mean Nusselt number change is negligible. The mean Nusselt number for the cavity with partitions is nearly the same as that evaluated for the simple cavity without partitions. However, for cavities with aspect ratios lower than indicated by the conduction-multicellular boundary (multicellular regime), the cavity mean Nusselt number reduction, resulting from partition presence, is obvious. The wider the cavity is, the greater the effect of partitions on the total heat-transfer reduction.

The results of calculations for corresponding peak Nusselt numbers in the cavity with partitions and for $Gr_H = 1 \times 10^8$, are depicted in Figure 7. As the comparison of Figures 2 and 7 for various aspect ratios suggests, the peak Nusselt number is also noticeably affected by partitions primarily in wider cavity in which the multicellular regime exists. In addition, Figure 7 also suggests that the peak Nusselt number depends

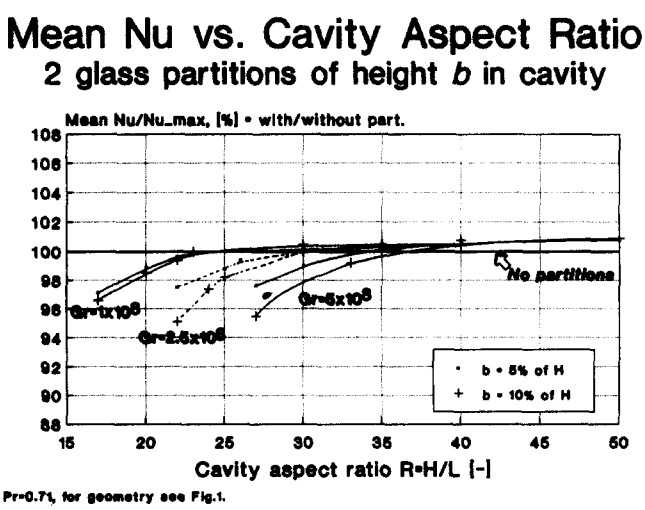

Figure 6 Mean Nusselt number in the cavity with two vertical partitions located in the middle of the opposite adiabatic walls

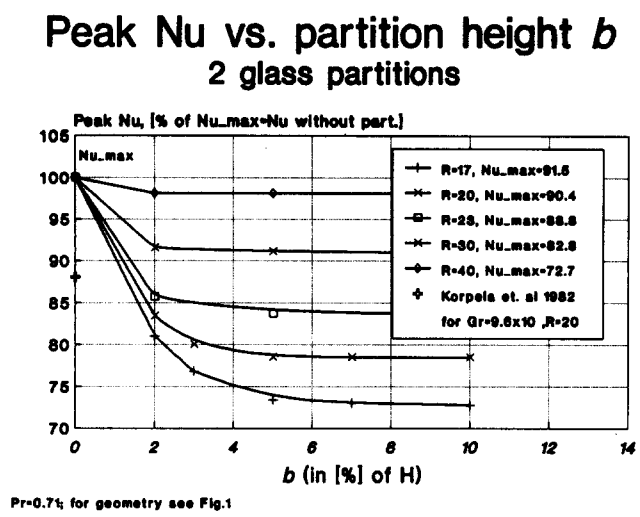

Figure 7 The effect of variable height, b, of partitions on the peak Nusselt number for $Gr = 1.0 \times 10^8$

strongly on the partition height, b, approximately for $b \leq 5$ percent of H. Calculations confirmed that these conclusions are valid for all Grashof numbers considered.

Finally, evaluated peak Nusselt numbers, for the range of aspect ratios and the Grashof numbers investigated, are depicted in Figure 8. In this figure, the ratio of Nu/Nu_{max} (the ratio of the peak Nusselt number in the cavity with two partitions and the peak Nusselt number in the same cavity without partitions) is depicted as a function of the cavity aspect ratio, $R = H/L$. Grashof number, Gr, is a parameter for each curve. For each Grashof number, just one curve is used to represent the peak Nusselt numbers for the variable heights of partitions, b, in the range of $5 \leq b \leq 20$ percent of H. The reason is that for $b \geq 5$ percent of H the peak Nusselt number value remains nearly unchanged regardless of the partition height (see Figure 7). Again, for all Grashof numbers investigated, the comparison of Figures 2 and 8 shows that partitions appreciably reduce the peak Nusselt numbers, especially in cavities with existing multicellular fluid-flow regime. However, in very narrow cavities the effect of inner partitions on the peak Nusselt number suppression becomes very weak.

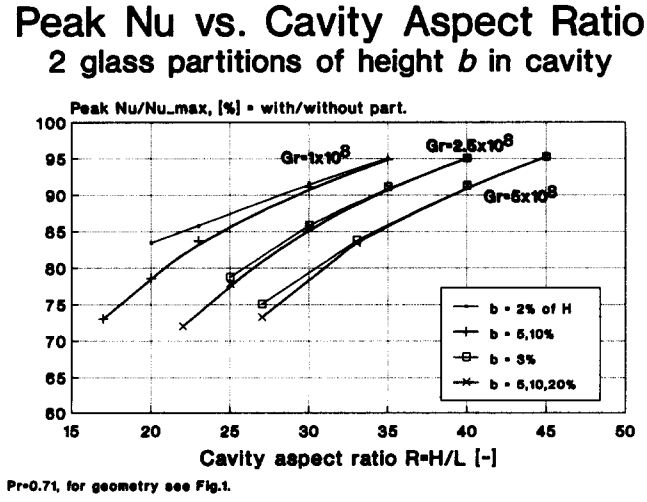

Figure 8 Peak Nusselt number in the cavity with two vertical partitions located in the middle of the opposite adiabatic walls

Conclusion

Heat transfer by natural convection in slender rectangular cavity with two thin glass partitions (convection barriers), located in the middle of cavity horizontal adiabatic walls (cavity top and bottom), was numerically investigated. Fluid-flow distribution, cavity mean Nusselt number and especially the peak Nusselt number values were determined. The following conclusions emerge:

1. Two small partitions can appreciably reduce the cavity peak Nusselt number values. This could be important especially for the double-paned window design, where the local heat-transfer performance could be meaningfully improved.
2. In both the conduction and multicellular regimes, resulting from the partition presence, the peak heat-transfer area is shifted from the top and bottom of the air cavity to the partition end.
3. Compared with the simple rectangular cavity without partitions, in the range of aspect ratios investigated, two small partitions decrease the cavity mean Nusselt number value by up to 6 percent provided that the fluid-flow regime is multicellular. In the conduction fluid-flow regime, the change of the mean Nusselt number, as the consequence of partition presence, is negligible.
4. Compared with the simple rectangular cavity without partitions in which the multicellular fluid-flow regime exists, if two small thin glass partitions, each of the height of 5 percent of the total cavity height, are located in the middle of cavity end walls, then the peak Nusselt number is decreased approximately by 20 percent. In reality, lower heat transfer from the room air to the window cavity, in the area where the cavity heat-transfer peak exists, will cause a lower temperature drop between the room air and the inner window pane. Consequently, a significant reduction of the condensation formation on this window pane will be achieved.

Acknowledgment

The authors gratefully acknowledge the financial support from the Renewable Energy Branch of the Department of Energy, Mines and Resources, Canada.

References

Bajorek, S. M. and Lloyd, J. R. 1982. Experimental investigation of natural convection in partitioned enclosure. *J. Heat Transfer*, **104**, 527

Bejan, A. 1982. Natural convection heat transfer in porous layer with internal flow obstructions. *Int. J. Heat Mass Transfer*, **24**, 815–822

Bergholz, R. F. 1978. Instability of steady natural convection in a vertical fluid layer. *ASME J. Heat Transfer*, **84**, 743

Chu, H. N. S. and Churchill, S. W. 1977. The development and testing of a numerical method for computation of laminar natural convection in enclosures. *Computers and Chemical Engineering*, **1**, 103–108

Ciofalo, M. and Karayiannis, T. G. 1991. Natural convection heat transfer in a partially—or completely—partitioned vertical rectangular enclosure. *Int. J. Heat Mass Transfer*, **34**, 167–179

ElSherbiny, S. M, Raithby, G. D. and Hollands, K. G. T. 1982. Heat transfer by natural convection across vertical and inclined air layers. *ASME J. Heat Transfer*, **104**, 159–167

Frederick, R. L. 1989. Natural convection in an inclined square enclosure with a partition attached to its cold wall. *Int. J. Heat Mass Transfer*, **32**, 87–94

Frederick, R. L. and Valencia, A. 1989. Heat transfer in a square cavity with a conduction partition on its hot wall. *Int. Commun. Heat Mass Transfer*, **16**, 347–354

Jetli, R. and Acharya, S. 1988. End wall effects on thermal stratification and heat transfer in a vertical enclosure with offset partitions. *Canadian J. Chem. Eng.*, **66**, 563–571

Korpela, S. A., Lee, Y. and Drummond, J. E. 1982. Heat transfer through a double paned window. *ASME J. Heat Transfer*, **104**, 539–544

Lee, Y. and Korpela, S. A. 1983. Multicellular natural convection in a vertical slot. *J. Fluid Mechanics*, **126**, 91–121

Newell, M. E. and Schmidt, F. W. 1970. Heat transfer by natural convection within rectangular enclosures. *ASME J. Heat Transfer*, **92C**, 159–167

Novak, M. H. and Nowak, E. S. 1993. Natural convection heat transfer in slender window cavities. *ASME J. Heat Transfer*. **115**, 476–479

Oosthuizen, P. H and Paul, J. T. 1985. Free convection heat transfer in a cavity fitted with a horizontal plate on the cold wall. *Advances in Enhanced Heat Transfer—1985*, ASME HTD, **43**, 101–107

Phillips, T. N. 1984. Natural convection in an enclosed cavity. *Journal of Computational Physics*, **54**, 365–381

Scozia, R. and Frederick, R. L. 1991. Natural convection in slender cavities with multiple fins attached to an active wall. *Numerical Heat Transfer*, **20**, 127–158

Shakerin, S., Bohn, M. and Loehrke, R. I. 1986. Natural convection in an enclosure with discrete roughness elements on a vertical heated wall. *Proc. 8th International Heat Transfer Conference*, **4**, 1519–1525

Wilkes, J. O. and Churchill, S. W. 1966. The finite-difference computation of natural convection in a rectangular enclosure. *AIChE J.*, **12**, 161–168

Zimmerman, E. and Acharya, S. 1987. Free convection heat transfer in partially divided vertical enclosure with conducting end walls. *Int. J. Heat Mass Transfer*, **30**, 319–331